Removal of ghost images by using tilted element optical systems with polynomial surfaces for aberration compensation

Jeremy D. Rogers, Tomasz S. Tkaczyk, and Michael R. Descour

College of Optical Sciences, University of Arizona, 1630 East University Boulevard, Tucson, Arizona 85721

Ari H. O. Kärkkäinen

Braggone Oy, Kaitovayla 1, FIN-90570 Oulu, Finland

Rebecca Richards-Kortum

Department of Bioengineering, Rice University, 6100 Main Street, Houston, Texas 77005

Received October 11, 2005; accepted November 12, 2005; posted November 16, 2005 (Doc. ID 65269)

A novel solution to problematic ghost images is implemented by using tilted lens elements with polynomial surfaces. Tilting the lens surfaces sends reflections out of the imaging path. The nonrotationally symmetric polynomial surfaces correct aberrations caused by tilts. The complex lens surfaces are fabricated by using gray-scale lithographic patterning of hybrid solgel glass. © 2006 Optical Society of America

OCIS codes: 220.3620, 220.1000.

Ghost images and stray light are particularly problematic in imaging applications where a large range of light levels exists. In astronomy the problem arises because of the extreme dynamic range involved in imaging bright and dim objects simultaneously. The light from a bright star can reflect and scatter from multiple elements and cause a faint ghost image that disrupts imaging of faint objects. In microscopy the problem arises when a bright source is used to illuminate a weakly reflective object through the imaging optics, as with epi-illumination. Antireflection (AR) coatings work well for reducing the reflections but cannot eliminate them completely. An alternative for suppressing ghost images is to tilt lenses such that the reflected light is sent out of the optical path and does not reach the detector or image plane. The method of stray light removal by tilted or decentered lenses was first formally discussed by Buchroeder.[1] A limitation of this design method is that tilted or decentered optics introduce aberrations that are difficult to correct by using spherical lenses. Typically, more elements are needed, and higher-order aberrations are controlled by balancing with third-order aberrations.

In this Letter we show that the aberrations can be eliminated by using nonrotationally symmetric lens surfaces that correct the wavefront error at each surface of power. This requires no more elements than the rotationally symmetric design and corrects the wavefront error directly without the need to balance third-order aberrations. The precise fabrication of small irregular lens surfaces has recently been made practical by technological advances in gray-scale lithography.[2] Other technologies such as diamond turning and injection molding have the potential to work for larger lenses. Our research utilizes gray-scale lithographic patterning of hybrid solgel glass,[3] and this is the technique we used to fabricate the system reported here. In this Letter we present an example design and the resulting reduction of ghost images from a modeled system as well as the measured improvement from a fabricated system.

During the development of a miniature microscope for detection of precancer,[4] ghost images and reflections were determined to severely limit the useful application of the device. Despite the use of AR coatings, the light reflected from a thin layer of cells was only a fraction of a percent of the incident light, and lens surface reflections dominated the image. As a measurement of the reflected signal from cell samples, a comparison was made by imaging a gold-labeled tissue phantom[5] in immersion and an uncoated glass surface in immersion. The Fresnel reflection from a glass surface in water is calculated to be less than 0.4%, and the image plane irradiance for the tissue was measured to be almost identical to that of the glass slide. However, the reflected signal from the in-focus cells must be even less, since the tissue reflects light from several hundred micrometers of depth, but only a thin layer of a few micrometers is in focus at a given time. With the structured illumination method[6,7] the maximum contrast of the grating projected into the tissue phantom is measured to be 12% of the reflected light. We therefore estimate the maximum reflectance from the in-focus

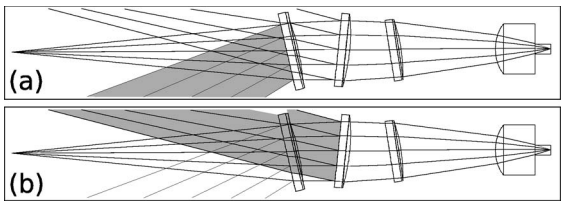

Fig. 1. Optical design: illumination rays (originating on-axis from the left) and reflected rays (shaded) are sent out of the system into baffles. For simplicity, only the reflected rays from (a) the first surface and (b) the third surface are shown. The device works in immersion, and the medium on the far right is water.

0146-9592/06/040504-3/$15.00

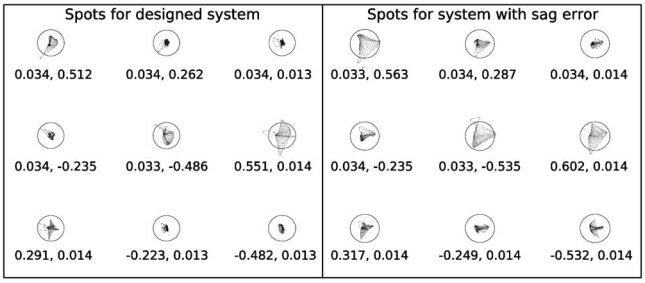

Fig. 2. Left is the spot diagram for the tilted component system. Right is the spot diagram for the worst-case 5% fabrication scaling error. The circles represent the size of the Airy disk with diameter 7.8 μm. The image points range from ±0.5 mm in both X and Y directions and represent the imaging of tissue at the detector ($m=-4$).

cells to be 12% of 0.4%, or 0.05% of the incident light. Simple AR coatings alone cannot reduce the surface reflections enough to allow imaging of such an object without further reduction of ghost reflections.

The use of gray-scale patterning to shape lenses for our device makes fabrication of arbitrary surfaces no more difficult than spherical surfaces, which facilitates a unique solution to the ghost image problem. Each lens element is tilted so that the reflection is directed out of the optical path as shown in Fig. 1. These tilts introduce aberrations that are corrected by fabricating asymmetric lens surfaces. The restriction of this scheme is that the gray-scale patterning technique imposes a limit on the sag of the lens surface. In a rotationally symmetric design, the sag limit constrains the f-number or the optical power of each lens for a given diameter. In a tilted component design some of the sag must also be used in the correction of aberrations. The challenge is then to minimize the tilt of each element while still removing the reflections from the image plane. This method will maximize the sag available for power in each element.

The tilted component system is designed in stages of increasing complexity. The first step is to design the optimal rotationally symmetric system. Required tilts can be estimated by sequentially treating each surface as a mirror and examining the beam footprint back at the starting plane. Next, the estimated tilts are introduced and a polynomial function is added to each surface. The polynomial coefficients are varied during optimization, with care taken to ensure that the surface function does not dip below the level of the substrate or exceed the maximum allowed sag for the component. Finally, a nonsequential ray trace is used to determine the actual size, strength, and location of reflections. The simulated overlap of reflections with the image plane can be used to iteratively fine tune the tilts needed to completely remove the reflection from a given surface.

Some reflections cannot be removed from the image plane without excessive tilts. This case occurs when the reflection from a curved surface results in a rapidly diverging beam. A tilt approaching 90° could be required in order to completely remove such a reflection. Note, however, that such a rapidly diverging beam will have a very large footprint at the image plane and will therefore have a very low energy density. It follows that the brightest reflections will tend to be the ones with the smallest spatial extent near the image plane. This is fortunate because these reflections require the smallest tilts in order to be completely removed from the image plane.

Once the tilts have been introduced, the surfaces can be modified to correct the aberrations. A biconic may be enough to correct the aberrations in some systems, but a third-order polynomial was used in our design, which provides more degrees of freedom. Equation (1) represents the surface function of the lenses, where each of the coefficients is varied during optimization:

$$z(x,y) = \frac{c(x^2+y^2)}{1+\sqrt{1-(1+k)c^2(x^2+y^2)}} + a_1x + a_2y + a_3x^2 + a_4xy + a_5y^2 + a_6x^3 + a_7x^2y + a_8xy^2 + a_9y^3. \quad (1)$$

In our case the result of this design process was a diffraction-limited system with a Strehl ratio above 0.8 over the entire field of view. Figure 2 shows the spot diagram for a selection of field points.

Such an unconventional optical design deserves a brief discussion of tolerances. Since the lens surfaces contain polynomial functions, it is reasonable to expect that the positional tolerance on these surfaces could be much tighter than for rotationally symmetric equivalent designs. A more thorough investigation of tolerances is needed, but initial results show that decentering of the lenses by up to 5 μm does not significantly degrade performance. This displacement is greater than the error in assembly using our current technology.[4] Another mode of fabrication error is an incorrect sag of the entire lens surface due to variations in the lithography exposure and development stages. This error is typically less than 5% and is seen as a linear scaling factor of the entire surface

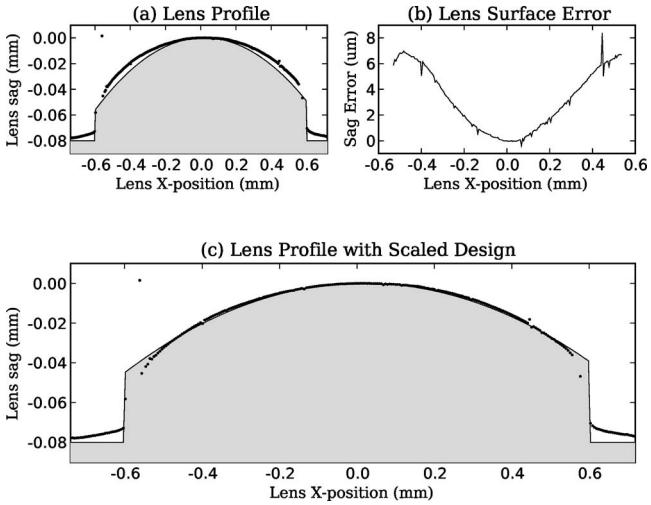

Fig. 3. Lens surface profile along the x axis, showing (a) both the designed profile (gray) and the fabricated surface (black points) as measured with a Wyko optical profilometer, (b) the fabrication error, and (c) the designed profile linearly scaled to match the fabricated lens surface.

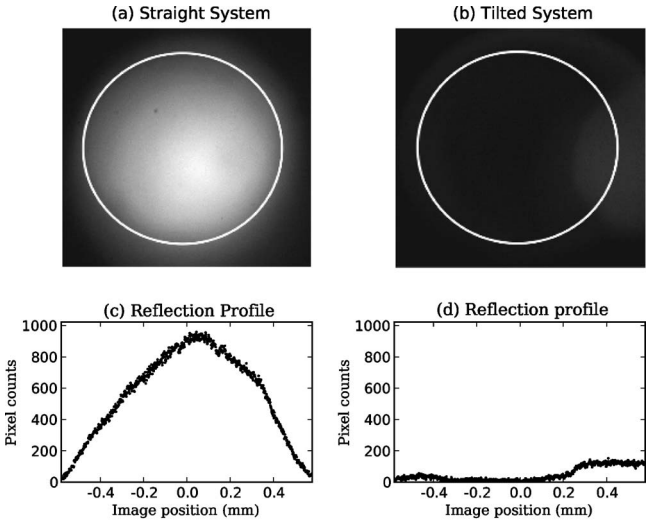

Fig. 4. Ghost images formed by (a) an untilted conventional system and (b) a tilted-component system. The circles depict the designed field of view (radius 0.5 mm at the image) for the system. In the tilted system, a faint ghost is visible on the right, just overlapping with the field of view.

function as shown in Fig. 3(c). Analysis of the effect on image quality shows that compensating with some defocus maintains the diffraction-limited performance for this design (Fig. 2).

Fabrication of the designed surfaces is not significantly different from that previously reported for symmetric lens systems.[8] The fabricated surface profile is measured with a Veeco NT3000 optical profilometer. The designed surface is plotted along with the measured profile in Fig. 3. The surface fabrication error is highly process dependent, but, when process parameters are tuned properly, the primary fabrication error is a linear scaling of the surface function as mentioned above. This error is most likely due to overdevelopment or underdevelopment of the exposed hybrid solgel glass. Since the fabrication process can be tuned to produce surface heights proportional to mask optical density, overdevelopment or underdevelopment will simply expand or shrink the surface function. This effect is shown in Fig. 3(c), where a scaled version of the designed surface function closely matches the fabricated surface.

The nonsequential ray-trace analysis of the design predicted a 75% reduction of stray light in the image plane. Measured reflections from the actual device, reduced by 85%, are consistent with the limitations of the model. Figure 4 shows a side-by-side comparison of a system with untilted rotationally symmetric lenses and a tilted component system. Both systems employ AR-coated lenses (V coat centered at 635 nm), and both images were taken with the same exposure time and illumination power. No object was placed at the object plane, so all light in the image is due to reflections from the lens elements.

This reduction in ghost images allowed us, for the first time, to image the tissue samples in reflectance. Work will now continue toward development of a miniature microscope for *in vivo* imaging and cancer detection. The general method of using tilts has potentially useful application in any system where ghost images are problematic and asymmetric lenses can be fabricated.

Research was funded by the National Institute of Biomedical Imaging and Bioengineering, grant EB002165. J. D. Rogers' e-mail address is jdrogers@optics.arizona.edu.

References

1. R. A. Buchroeder, "Tilted component optical systems," Ph.D. dissertation (University of Arizona, 1976).
2. A. H. O. Kärkkäinen, J. T. Rantala, and M. R. Descour, Electron. Lett. **38**, 23 (2002).
3. A. H. O. Kärkkäinen, J. T. Rantala, A. Maaninen, G. E. Jabbour, and M. R. Descour, Adv. Mater. **14**, 535 (2002).
4. M. R. Descour, A. H. O. Kärkkäinen, J. D. Rogers, C. Liang, R. S. Weinstein, J. T. Rantala, B. Kilic, E. Madenci, R. R. Richards-Kortum, E. V. Anslyn, R. D. Dupuis, R. J. Schul, C. G. Willison, and C. P. Tiggis, IEEE J. Quantum Electron. **38**, 122 (2002).
5. K. Sokolov, M. Follen, J. Aaron, I. Pavlova, A. Malpica, R. Lotan, and R. Richards-Kortum, Cancer Res. **63** 1999 (2003).
6. M. A. Neil, R. Juskaitis, and T. Wilson, Opt. Lett. **22**, 1905 (1997).
7. T. S. Tkaczyk, M. Rahman, V. Mack, K. Sokolov, J. D. Rogers, R. Richards-Kortum, and M. R. Descour, Opt. Express **12**, 3745 (2004).
8. J. D. Rogers, A. H. O. Kärkkäinen, T. Tkaczyk, J. T. Rantala, and M. Descour, Opt. Express **12**, 1294 (2004).